LBL-38245
UC-404

Lawrence Berkeley Laboratory
UNIVERSITY OF CALIFORNIA

Accelerator & Fusion
Research Division

Long Wavelength End-Effect Undulator Radiation (Transition Undulator Radiation)

B.M. Kincaid

January 1996

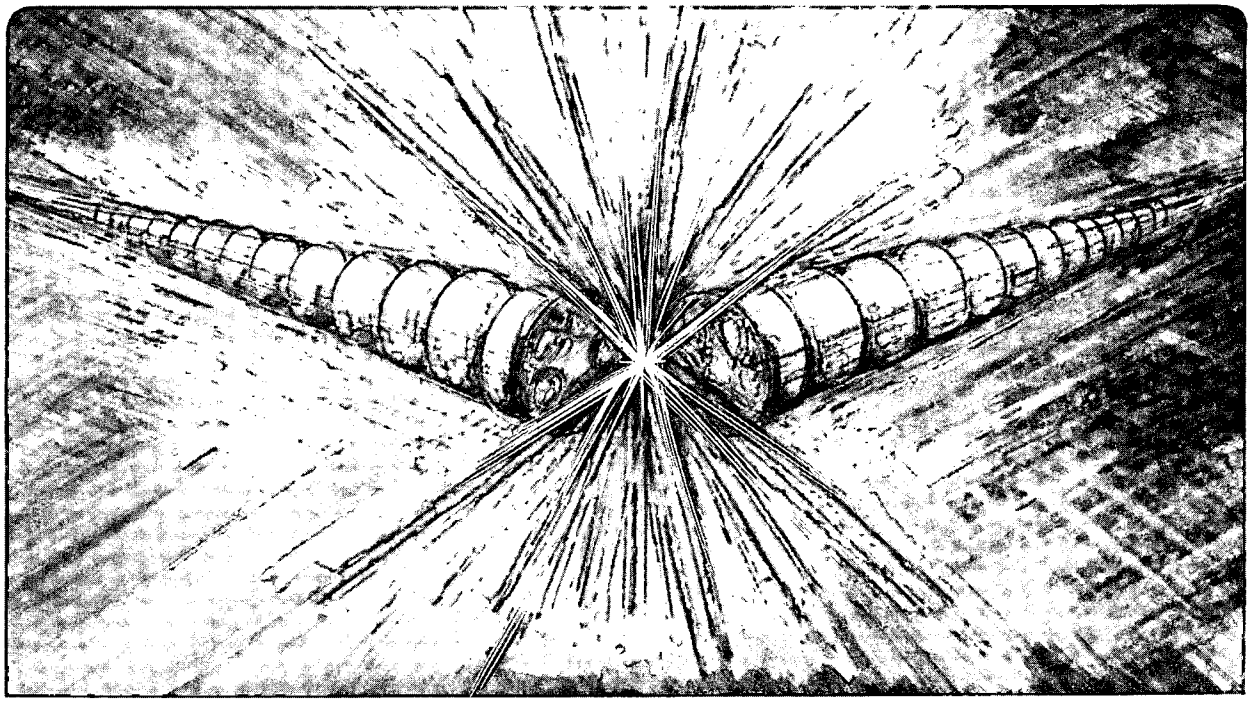

Prepared for the U.S. Department of Energy under Contract Number DE-AC03-76SF00098

DISCLAIMER

LBL-38245

Long Wavelength End-Effect Undulator radiation (Transition Undulator Radiation)*

Brian M. Kincaid

Advanced Light Source
Accelerator and Fusion Research Division
Lawrence Berkeley National Laboratory
University of California
Berkeley, CA 94720

January 29, 1996

*This work was supported by the Director, Office of Energy Research, Office of Basic Energy Sciences, Materials Sciences Division of the U.S. Department of Energy, under Contract No. DE-AC03-76SF00098

Long Wavelength End-Effect Undulator Radiation (Transition Undulator Radiation)†

BRIAN M. KINCAID

Ernest Orlando Lawrence Berkeley National Laboratory
1 Cyclotron Road, Berkeley, CA 94720

ABSTRACT

As first pointed out by K.-J. Kim [1] undulator radiation contains a broad-band component in the long wavelength region. This radiation is due to the change in longitudinal velocity of an electron upon entering and leaving an undulator. The radiation pattern is a hollow cone, peaked in the forward direction, with an opening angle of approximately $1/\gamma$, with a spectrum covering a wide range, including the infra-red and the visible. The radiation is radially polarized, analogous to transition radiation, and exhibits interference effects between the entrance and exit ends of the undulator, similar to the interference effects observed for transition radiation from a thin slab of material. A straightforward application of formulas from Jackson [2] results in a closed form exact expression for the low frequency limit of this novel radiation effect, Transition Undulator Radiation or TUR.

† This work was supported by the Director, Office of Energy Research, Office of Basic Energy Sciences, Materials Sciences Division, of the U. S. Department of Energy, under contract DE – AC03 – 76SF00098.

1. INTRODUCTION

TUR is produced by the change in longitudinal velocity occurring at the ends of an undulator. The electron enters the device with a velocity βc. The transverse deflection of the electron by the undulator magnetic field causes a change in the longitudinal velocity according to $\beta_z = \sqrt{\beta^2 - \beta_x^2 - \beta_y^2}$, since, neglecting radiation losses, the energy of the electron is not changed by the magnetic field. For the case of a planar undulator, the β_z oscillates at twice the rate of the transverse motion, and has an average value given by

$$\beta^* = \sqrt{1 - \frac{1}{\gamma^{*2}}}. \tag{1}$$

Here, γ^* is given by

$$\gamma^* = \frac{\gamma}{\sqrt{1 + K^2}}, \tag{2}$$

where K is calculated from the *effective* magnetic field strength.[3] For a planar undulator, for example, $K = K_{peak}/\sqrt{2}$.

Thus, for highly relativistic electrons, even though the value of β is close to unity and does not change very much upon entering the undulator, the effective γ changes quite a bit, especially in the case of large K undulators and wigglers.

We are concerned with low-frequency radiation effects, so we may average over the high-frequency oscillations in β_z, and the normal transverse motions β_x and β_y, which produce the conventional undulator radiation harmonics. The electron's motion in the z-direction consists of a deceleration at the undulator entrance followed by an acceleration at the device exit. These accelerations produce the TUR.

Another way to visualize the separation of the high frequency motion from the longitudinal motion responsible for TUR is to consider a high-K helical undulator, where β_x and β_y have the same amplitude. The transverse motion is the normal helical trajectory, while the longitudinal motion is exactly the deceleration and acceleration described above, without the assumption of averaging over the high frequency motion. The normal on-axis radiation consists of only the fundamental undulator frequency, and is circularly polarized. The higher undulator harmonics are radiated into a hollow cone with an opening angle of K/γ, and are also mainly circularly polarized. The TUR is confined to a hollow cone on axis with an opening angle of $1/\gamma$, and is radially polarized.

Henceforth, only the radiation produced by the longitudinal motion will be considered. The longitudinal accelerations are opposite in sign and similar in magnitude for a typical undulator, so the electron radiates a pulse of electric field at

the entrance to the device, followed by another pulse with opposite sign at the exit. In a moving frame, the electron emits a dipole radiation pattern which, when viewed in the lab frame, is transformed into a radially polarized hollow cone with an opening angle of $1/\gamma$. A distant observer therefore sees two pulses of electric field, of opposite sign and roughly equal magnitude, with source points separated in time and longitudinal distance. This gives rise to Fresnel zone-like ring interference patterns and a radiation spectrum at a fixed angle with periodic oscillations. Figure 1 shows this schematically.

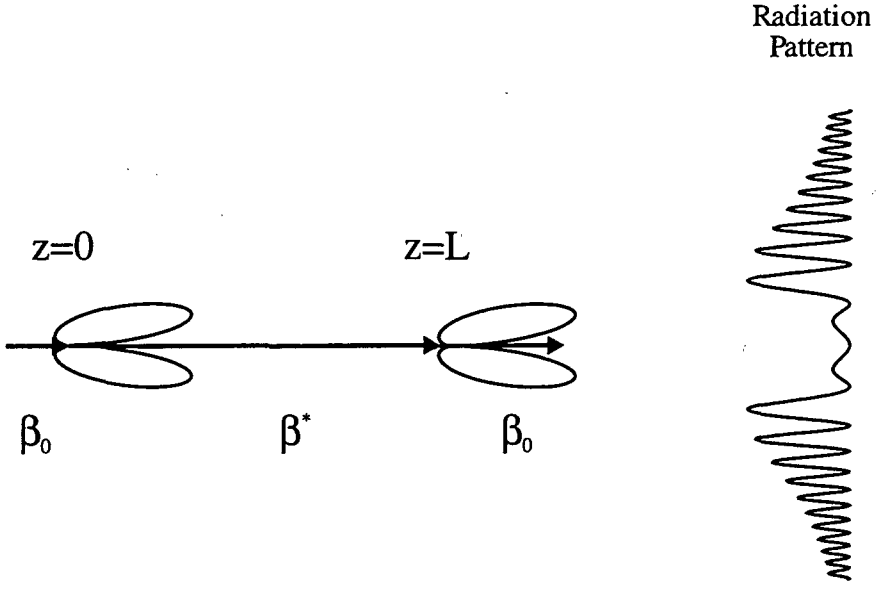

Figure 1.

2. Calculation of angular distribution of radiation spectrum

Starting with the expression for the energy radiated by a single electron per unit solid angle and frequency (Jackson 14.67),

$$\frac{d^2I}{d\omega d\Omega} = \frac{e^2}{4\pi^2 c}\left|\int_{-\infty}^{+\infty} \frac{\hat{\mathbf{n}}\times(\hat{\mathbf{n}}-\boldsymbol{\beta})\times\dot{\boldsymbol{\beta}}}{(1-\hat{\mathbf{n}}\cdot\boldsymbol{\beta})^2} e^{+i\omega\left(t-\frac{\hat{\mathbf{n}}\cdot\mathbf{r}(t)}{c}\right)}dt\right|^2 . \tag{3}$$

Using Jackson (14.66), the integrand, excluding the exponential, is a perfect differential,

$$\frac{\hat{\mathbf{n}}\times[(\hat{\mathbf{n}}-\boldsymbol{\beta})\times\dot{\boldsymbol{\beta}}]}{(1-\hat{\mathbf{n}}\cdot\boldsymbol{\beta})^2} = \frac{d}{dt}\left[\frac{\hat{\mathbf{n}}\times(\hat{\mathbf{n}}\times\boldsymbol{\beta})}{1-\hat{\mathbf{n}}\cdot\boldsymbol{\beta}}\right]. \tag{4}$$

Substituting,

$$\frac{d^2I}{d\omega d\Omega} = \frac{e^2}{4\pi^2 c}\left|\int_{-\infty}^{+\infty}\frac{d}{dt}\left[\frac{\hat{\mathbf{n}}\times(\hat{\mathbf{n}}\times\boldsymbol{\beta})}{1-\hat{\mathbf{n}}\cdot\boldsymbol{\beta}}\right]e^{+i\omega\left(t-\frac{\hat{\mathbf{n}}\cdot\mathbf{r}(t)}{c}\right)}dt\right|^2 \tag{5}$$

This is Jackson (15.1).

Treating the entrance and exit motions separately, we can follow the treatment in Jackson, Chapter 15, covering the radiation emitted during collisions caused by a change in particle velocity. Separate expressions for the entrance and exit radiation pulses can be summed with the appropriate phase later. In the low frequency limit, $\omega \to 0$, the exponential factor is a constant equal to unity. The integrand is then a perfect differential, and therefore the spectrum of radiation with polarization ϵ is

$$\lim_{\omega\to 0}\frac{d^2I}{d\omega d\Omega} = \frac{e^2}{4\pi^2 c}\left|\boldsymbol{\epsilon}^*\cdot\left(\frac{\boldsymbol{\beta}_2}{1-\hat{\mathbf{n}}\cdot\boldsymbol{\beta}_2}-\frac{\boldsymbol{\beta}_1}{1-\hat{\mathbf{n}}\cdot\boldsymbol{\beta}_1}\right)\right|^2 \tag{6}$$

Here $\boldsymbol{\beta}_2$ is the velocity after the acceleration (deceleration) and $\boldsymbol{\beta}_1$ is the initial velocity, and $\boldsymbol{\epsilon}^*$ is the (complex conjugate) polarization vector.

Since the accelerations are longitudinal, $\boldsymbol{\beta} = \beta\hat{\mathbf{z}}$. If the angle between $\hat{\mathbf{n}}$ and $\boldsymbol{\beta}$ is θ, then $\boldsymbol{\epsilon}\cdot\boldsymbol{\beta} = \beta\sin\theta \approx \beta\theta$, and

$$\lim_{\omega\to 0}\frac{d^2I}{d\omega d\Omega} = \frac{e^2}{4\pi^2 c}\left(\frac{\beta_2\theta}{1-\beta_2\cos\theta}-\frac{\beta_1\theta}{1-\beta_1\cos\theta}\right)^2. \tag{7}$$

$$1-\beta_1\cos\theta \approx 1-\left(1-\frac{1}{2\gamma^2}\right)\left(1-\frac{\theta^2}{2}\right) \approx \frac{1+\gamma^2\theta^2}{2\gamma^2} \tag{8}$$

$$1-\beta_2\cos\theta \approx 1-\left(1-\frac{1}{2\gamma^{*2}}\right)\left(1-\frac{\theta^2}{2}\right) \approx \frac{1+\gamma^{*2}\theta^2}{2\gamma^{*2}} \tag{9}$$

This gives

$$\lim_{\omega\to 0}\frac{d^2I}{d\omega d\Omega} = \frac{e^2}{4\pi^2 c}\left(\frac{2\gamma^2K^2\theta}{(1+K^2+\gamma^2\theta^2)(1+\gamma^2\theta^2)}\right)^2. \tag{10}$$

In the usual units, $(photons/sec/mrad^2/0.1\%\Delta\omega/\omega)$,

$$\lim_{\omega\to 0}\frac{d^2N}{d\omega/\omega d\Omega} = 10^{-9}\times\frac{\alpha}{4\pi^2}\left(\frac{I}{e}\right)\left(\frac{2\gamma^2K^2\theta}{(1+K^2+\gamma^2\theta^2)(1+\gamma^2\theta^2)}\right)^2. \tag{11}$$

Here α is the fine structure constant and (I/e) is the number of particles per second in the electron beam. The expression peaks at $\gamma\theta \approx 1/\sqrt{3}$ for small K and at $\gamma\theta \approx 1$ for large K. Also note that the expression is independent of K for large K.

3. INTERFERENCE EFFECTS

For a single electron, a distant observer sees two electromagnetic wave pulses, one from the entrance end of the undulator and another from the exit end. These pulses are similar in size and shape and opposite in sign. As shown in Figure 2, the time difference between the two pulses at the distant observer at an angle θ is given by

$$c\Delta t = \frac{L}{\beta^*} - L\cos\theta. \tag{12}$$

Here the first term is the time-of-flight of the electron from the entrance to the exit of the undulator, where the second pulse is emitted, and the second term is the time for light to travel the length of the undulator.

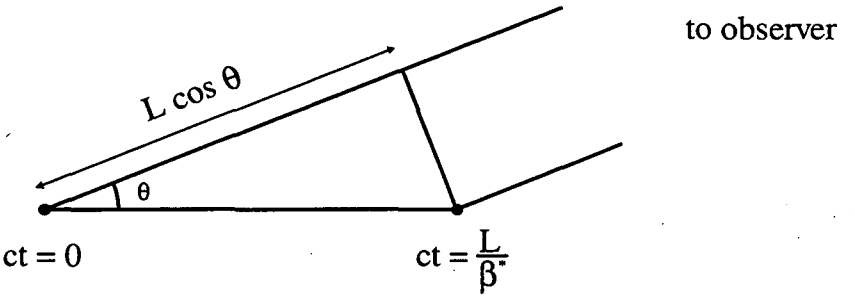

Figure 2.

Using the same small angle and large γ approximations as before,

$$c\Delta t = \frac{L}{2\gamma^2}(1 + K^2 + \gamma^2\theta^2). \tag{13}$$

If the electric field pulse emitted is described by $E(t)$, then the observer detects an intensity

$$I(\theta, t) \propto |E(t) - E(-t + \Delta t)|^2. \tag{14}$$

The sign of the argument of the second term is due to the time reversed nature of the accelerations at the ends of the undulator. In terms of the photon irradiance spectrum,

$$\lim_{\omega\to 0} \frac{d^2N}{d\omega/\omega d\Omega} = \frac{\alpha}{4\pi^2}\left(\frac{I}{e}\right)\left(\frac{2\gamma^2K^2\theta}{(1 + K^2 + \gamma^2\theta^2)(1 + \gamma^2\theta^2)}\right)^2 \times 4\sin^2\frac{\omega\Delta t}{2}. \tag{15}$$

The θ dependence of Δt gives rise to Fresnel zone-like interference rings. As long as the frequency ω is not too large, the expression for the low-frequency limit is

a good approximation, and for fixed θ, the spectrum oscillates from zero to four times the single pulse value. The detailed shape of the electric field pulses, and hence the detailed ω dependence of the spectrum are not produced by the above analysis, since only the low-frequency limit has been examined. For real insertion devices, the calculated spectrum is relatively constant from the far infrared well into the visible.

4. Comparison with bending magnet (BM) radiation

The photon irradiance spectrum from a BM source is

$$\frac{d^2N}{d\omega/\omega d\Omega} = \frac{3\alpha}{4\pi^2}\gamma^2 \left(\frac{I}{e}\right) H_2(y), \tag{16}$$

where $H_2(y) = y^2 K_{2/3}^2(y/2)$, and $y = \omega/\omega_c$, as usual. The ratio of TUR to BM radiation is given by

$$R = \frac{8}{3H_2(y)} \frac{\gamma^2\theta^2 K^4}{(1+K^2+\gamma^2\theta^2)^2(1+\gamma^2\theta^2)^2} \tag{17}$$

For simplicity, the $\sin^2$ term has been replaced by it's average value of $1/2$, as discussed further in the next section. Since the maximum value of

$$\frac{\gamma^2\theta^2 K^4}{(1+K^2+\gamma^2\theta^2)^2(1+\gamma^2\theta^2)^2} \tag{18}$$

is $1/4$, the maximum value of R is given by

$$R = \frac{2}{3H_2(y)}. \tag{19}$$

For $0.001 < y < 1$, $.03 < H_2(y) < 1.47$, so TUR can have approximately one order of magnitude larger irradiance than BM radiation. In practice, however, this may be difficult to observe, since the fringe field region of the bend magnets upstream and downstream of the undulator produce a spectrum with a much lower critical energy than the full bend field. This increases the amount of low-frequency radiation produced by the bend magnets, and hence reduces the ratio of TUR to BM radiation.

5. TOTAL FLUX

To determine the total flux for a given ω, integrate over solid angle,

$$\lim_{\omega \to 0} \frac{dN}{d\omega/\omega} = 2\pi \int_0^{\pi} \frac{d^2N}{d\omega/\omega d\Omega} \sin\theta d\theta. \tag{20}$$

Since the radiation pattern is confined to small angles, this may be approximated by

$$\lim_{\omega \to 0} \frac{dN}{d\omega/\omega} = 2\pi \int_0^{\infty} \frac{d^2N}{d\omega/\omega d\Omega} \theta d\theta. \tag{21}$$

Changing the integration variable to $u = \gamma^2\theta^2$,

$$\lim_{\omega \to 0} \frac{dN}{d\omega/\omega} = \frac{4\alpha}{\pi}\left(\frac{I}{e}\right) \int_0^{\infty} \frac{K^4 u}{(1+K^2+u)^2(1+u)^2} \sin^2(\omega L(1+K^2+u)/2\gamma^2 c) du. \tag{22}$$

If ω is large enough for there to be a significant number of interference zones in the radiation pattern, the $\sin^2$ term can be approximated by it's average value of $1/2$. Evaluating the definite integral, (22) becomes

$$\lim_{\omega \to 0} \frac{dN}{d\omega/\omega} = \frac{2\alpha}{\pi}\left(\frac{I}{e}\right)\left(-2 + \log(1+K^2) + \frac{2\log(1+K^2)}{K^2}\right). \tag{23}$$

For small K, this expression is approximately

$$\lim_{\omega \to 0} \frac{dN}{d\omega/\omega} = \frac{\alpha}{3\pi}\left(\frac{I}{e}\right) K^4. \tag{24}$$

As shown in Figure 3, even though the expression diverges logarithmically for large K, for normal values of K it is quite well behaved. For $K = 1$ the K^4 approximation is already incorrect by a factor of two. For K up to about 30 the value of the K-dependent part of (23) is on the order of three.

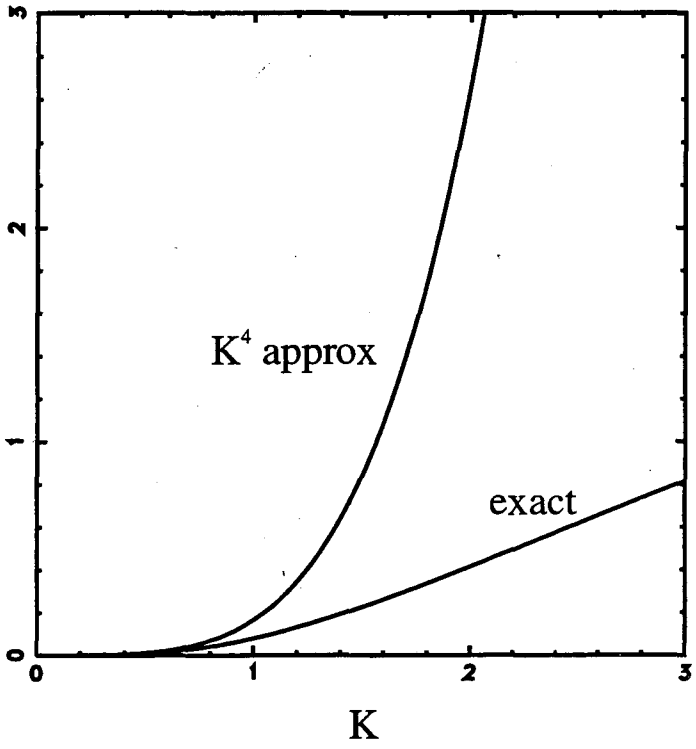

Figure 3.

6. Comparison with BM radiation

The flux integrated over vertical angle emitted from a BM source is

$$\frac{d^2N}{d\omega/\omega d\theta} = \frac{\sqrt{3}}{2\pi}\alpha\gamma\left(\frac{I}{e}\right)G_1(y), \tag{25}$$

where

$$G_1(y) = y\int_y^\infty K_{5/3}(y')dy'. \tag{26}$$

Integrating over a horizontal angle of approximately $1/\gamma$, the ratio of TUR to the flux from the BM source is approximately $7/G_1(y)$. If one is observing BM radiation from the fringe field region of the magnet, $G_1(y)$ can be significant, possibly near unity. This says that under these conditions, total flux from TUR may be only marginally greater than that from BM radiation. However, depending on the details of the fringe field of the BM, and depending on ω, the ratio may be significantly larger. Of course, a larger horizontal collection angle for the BM radiation will reduce this ratio. It should be noted that for long wavelengths, the

vertical opening angle of BM radiation can be significantly larger than $1/\gamma$. This says that TUR is more concentrated in the forward direction than BM radiation, but that the total flux is comparable to what is achievable using BM sources and large collection angles.

7. Conclusion

TUR is an interesting effect, and may produce marginally more irradiance and flux than BM sources. The exact details of the fringe field region of upstream and downstream bend magnets makes the possible advantage of TUR difficult to predict, and measurements should be done. Some work has been done predicting total power radiated in the fringe field region,[3] and this could be expanded to improve the estimates used above.

M. R. Howells has pointed out that TUR fringe patterns may have some use as a electron beam diagnostic. The number of fringes, their contrast, alignment, etc., may give some useful information about things like energy and angular spread of the electron beam or the trajectory of the beam through the undulator.

Helpful conversations with M. R. Howells are gratefully acknowledged.

REFERENCES

1. K.-J. Kim, accepted for publication in Physical Review Letters, 1996.
2. J. D. Jackson, *Classical Electrodynamics*, Second Edition, J. Wiley & Sons, NY 1975.
3. M. R. Howells and B. M. Kincaid, "The properties of undulator radiation", in *New Directions in Research with Third-Generation Soft X-Ray Synchrotron Radiation Sources*, A. S. Schlachter and F. J. Wuilleumier, eds., NATO ASI Series E, Vol. 254, Kluwer Academic Publishers, Dordrecht, The Netherlands 1994.

LAWRENCE BERKELEY NATIONAL LABORATORY
UNIVERSITY OF CALIFORNIA
TECHNICAL & ELECTRONIC INFORMATION DEPARTMENT
BERKELEY, CALIFORNIA 94720